Laser and Particle Beams (2017), *35*, 631–640.

doi:10.1017/S0263034617000581

Evolution of a circularly polarized laser beam in an obliquely magnetized plasma channel

HEMLATA,[1] A.K. UPADHYAY,[2] AND P. JHA[1]

[1]Department of Physics, University of Lucknow, Lucknow 226007, India
[2]Department of Applied Science, Teerthanker Mahaveer University, Moradabad 244001, India

(RECEIVED 15 May 2017; ACCEPTED 17 August 2017)

Abstract

The evolution of the spot size and amplitude of a circularly polarized laser beam propagating in a plasma channel embedded in an obliquely applied magnetic field has been investigated. The wave equation describing the evolution of the radiation field is set up and a variational technique is used to obtain the equations governing the evolution of the spot size and amplitude. Numerical methods are used to analyze the evolution of the laser beam spot size and amplitude. It is seen that the amplitudes of the two transverse components of the electric field of the laser beam evolve differently, since they are driven by unequal current densities. This leads to the conversion of a circularly polarized laser beam into an elliptically polarized beam, under appropriate conditions.

Keywords: Conversion of circular to elliptically polarized laser beam; Evolution of spot size and amplitude; Obliquely magnetized plasma channel

1. INTRODUCTION

Optical guiding of intense laser beams in plasma is beneficial for a variety of applications, including harmonic generation (Abdelli *et al.*, 1992; Nuzzo *et al.*, 2000), development of X-ray lasers (Amendt *et al.*, 1991; Eder *et al.*, 1994), advanced laser fusion schemes (Tabak *et al.*, 1994; Deutsch *et al.*, 1996) and plasma-based accelerators (Tajima & Dawson, 1979; Berezhiani & Murusidze, 1992; Esarey *et al.*, 1996). At high intensities the interaction between lasers and plasma becomes nonlinear. This leads to many interesting phenomena such as self-focusing (Shen, 1984; Esarey *et al.*, 1997), wakefield generation (Esarey *et al.*, 2009), magnetic field generation (Gorbunov *et al.*, 1997), and other parametric instabilities (Kaw *et al.*, 1973). To allow optimum laser–plasma interaction for the abovementioned applications, it is necessary that the laser beams should propagate several Rayleigh lengths in plasma. For this purpose, plasma channels have been proposed for extending the propagation distance of laser beams.

Jha *et al.*, (2006, 2007) have studied the enhancement of self-focusing of an intense laser beam propagating in plasma embedded in transverse as well as axial magnetic fields. Magnetic fields applied or generated, not only help in guiding laser beams in plasma, but also lead to several interesting nonlinear phenomena and applications such as harmonic generation (Jha *et al.*, 2007.), THz radiation generation (Hu *et al.*, 2013; Wang *et al.*, 2015; Verma & Jha, 2016; Sharma *et al.*, 2017), and modulation instability (Jha *et al.*, 2005; Chen *et al.*, 2011). The effects of externally applied static magnetic field on wake excitation (Jha *et al.*, 2012) and non-linear evolution of laser pulses have been studied (Ren & Mori, 2004; Jha *et al.*, 2014).

Recently, a direct three-dimensional model for studying the effect of obliqueness of an externally applied magnetic field, on the characteristics of wakefields generated in magnetized plasma, has been reported (Manouchehrizadeh & Dorranian, 2013). Significant enhancement of the axial component of the generated wakefield and extinction of the radial components of plasma wakes occurs when the direction of the external magnetic field is appropriately varied. An analytical and numerical investigation for studying the wakefields driven by a short laser pulse in underdense plasma in the presence of a strong oblique DC magnetic field has been reported (Hu *et al.*, 2012). The abovementioned studies based on interaction of laser beams with obliquely magnetized plasma, has motivated the present study of the amplitude evolution of a circularly polarized laser beam propagating in an obliquely magnetized plasma channel.

Address correspondence and reprint requests to: Pallavi Jha, Department of Physics, University of Lucknow, Lucknow 226007, India. E-mail: prof.pjha@gmail.com

The organization of the paper is as follows: In Section 2, using perturbation technique, we have obtained the nonlinear current densities generated due to the propagation of an intense circularly polarized laser beam through obliquely magnetized plasma, in the mildly relativistic regime. In Section 3, non-paraxial equations for the evolution of the laser fields in a preformed, obliquely magnetized plasma channel are set up. The linear dispersion relations for the electric field components along the x- and y-directions have been derived. Lagrangian method has been used to obtain the evolution equations for the laser spot size and amplitude. In Section 4, numerical methods are used to graphically analyze the evolution of the laser spot size and amplitude of the x and y components of the electric field of the laser beam. Summary and conclusions are discussed in Section 5.

2. FORMULATION

Consider a circularly polarized laser beam propagating along the z-direction in a preformed plasma channel embedded in an obliquely applied magnetic field $\vec{b}_0(=\hat{y}b_0\sin\theta+\hat{z}b_0\cos\theta)$ lying in the y–z plane at an angle θ with respect to the z-axis. The radial profile of the plasma density is of the form $n_0(r)=n_{00}(1+\Delta n r^2/n_{00}r_{ch}^2)$, where n_{00} is the ambient, on-axis, plasma electron density, while r_{ch} and Δn are the channel radius and depth, respectively. The electric vector of the radiation field is given by

$$\vec{E}=E(r,z)\left\{\hat{x}\cos(k_0z-\omega_0t)-\sigma\hat{y}\sin(k_0z-\omega_0t)\right\}. \quad (1)$$

where $E(r, z)$, k_0, and ω_0 are the slowly varying amplitude, wave number and frequency of the laser electric field, respectively. σ takes the value ±1 for right or left circularly polarized radiation. The wave equation governing the propagation of the laser beam through plasma is given by

$$\left(\nabla^2-\frac{1}{c^2}\frac{\partial^2}{\partial t^2}\right)\vec{E}=\frac{4\pi}{c^2}\frac{\partial\vec{J}}{\partial t}. \quad (2)$$

The plasma current density may be obtained from

$$\vec{J}=-ne\vec{v}. \quad (3)$$

where $\vec{v}$ and n are, respectively, the plasma electron velocity and density. The equations governing the relativistic interaction between the electromagnetic field and plasma electrons are the Lorentz force equation

$$\frac{d(\gamma\vec{v})}{dt}=-\frac{e\vec{E}}{m}-\frac{e}{mc}\vec{v}\times\left(\vec{B}+\vec{b}_0\right) \quad (4)$$

and the equation of continuity

$$\frac{\partial n}{\partial t}+\vec{\nabla}.(n\vec{v})=0, \quad (5)$$

where $\gamma(=(1-v^2/c^2)^{-1/2})$ is the relativistic factor and $\vec{B}[=E(r,z)\left\{\sigma\hat{x}\sin(k_0z-\omega_0t)+\hat{y}\cos(k_0z-\omega_0t)\right\}]$ is the magnetic vector of the radiation field. It is assumed that the plasma electrons are at rest before the passage of the laser beam and therefore the external magnetic field does not affect them.

In order to study the evolution of the laser beam, in the mildly relativistic regime, the current density has to be obtained. This requires the derivation of perturbed velocities and density of plasma electrons. Using a perturbative technique all quantities are simultaneously expanded in orders of the radiation field. The first-order expansion of Eq. (4) leads to the equations governing the evolution of the plasma electron velocity components along the x, y, and z-directions, as

$$\frac{\partial v_{x,y}^{(1)}}{\partial t}=-\frac{e}{m}E_{x,y}-\frac{e}{mc}\left(\vec{v}^{(1)}\times\vec{b}_0\right)_{x,y} \quad (6a)$$

and

$$\frac{\partial v_z^{(1)}}{\partial t}=-\frac{e}{mc}\left(\vec{v}^{(1)}\times\vec{b}_0\right)_z. \quad (6b)$$

Simultaneous solution of Eqs (6a) and (6b) gives the first-order quiver velocity of the plasma electrons as

$$v_x^{(1)}=v_{0x}\sin(k_0z-\omega_0t), \quad (7a)$$

$$v_y^{(1)}=v_{0y}\cos(k_0z-\omega_0t) \quad (7b)$$

and

$$v_z^{(1)}=-v_{0z}\cos(k_0z-\omega_0t), \quad (7c)$$

where

$$v_{0x}\left(=\frac{ca\omega_0(\omega_0+\sigma\omega_c\cos\theta)}{(\omega_0^2-\omega_c^2)}\right)$$

and

$$v_{0y}\left(=\frac{\sigma ca\left\{\omega_0(\omega_0+\sigma\omega_c\cos\theta)-\omega_c^2\sin^2\theta\right\}}{(\omega_0^2-\omega_c^2)}\right)$$

are the amplitudes of the transverse quiver velocity components and

$$v_{0z}\left(=\frac{ca\omega_c\sin\theta(\omega_0+\sigma\omega_c\cos\theta)}{(\omega_0^2-\omega_c^2)}\right)$$

is the amplitude of the longitudinal velocity while $a(=eE/m\omega_0c)$ and $\omega_c(=eb_0/mc)$ are respectively the normalized radiation field amplitude and cyclotron frequency of the plasma electrons. Equations (7) show that application of the static magnetic field increases (decreases) the transverse

https://doi.org/10.1017/S0263034617000581 Published online by Cambridge University Press

quiver velocities of plasma electrons for $\sigma = +1(-1)$, for positive values of $\cos\theta$. Therefore, henceforth, $\sigma = +1$ (right circular polarization), has been considered. It is seen that the transverse quiver velocities are maximum when $\theta = 0°$ and reduce with increase in θ. Also it may be noted that the obliqueness of the applied external magnetic field leads to the generation of a new longitudinal velocity component. This velocity reduces to zero for the case of an axially magnetized plasma channel ($\theta = 0$).

Using Eq. (4), the second-order velocity components may be obtained from the following set of equations

$$\frac{\partial v^{(2)}_{x,y,z}}{\partial t} + v^{(1)}_z \frac{\partial v^{(1)}_{x,y,z}}{\partial z} = -\frac{e}{mc}\left(\vec{v}^{(1)} \times \vec{B}\right)_{x,y,z} - \frac{e}{mc}\left(\vec{v}^{(2)} \times \vec{b}_0\right)_{x,y,z}. \tag{8}$$

Substituting the first-order quantities from Eqs. (7), Eqs. (8) are solved to give

$$v^{(2)}_x = -\frac{c^2 a^2 \omega_c^2 k_0 \sin 2\theta}{8\omega_0^3} \sin 2(k_0 z - \omega_0 t), \tag{9a}$$

$$v^{(2)}_y = -\frac{c^2 a^2 \omega_c^2 k_0 \sin 2\theta}{8\omega_0^3} \cos 2(k_0 z - \omega_0 t) \tag{9b}$$

and

$$v^{(2)}_z = 0. \tag{9c}$$

While deriving Eq. (9), the cyclotron frequency of the plasma electron is considered to be much less than the frequency of the laser field. Therefore, third and higher powers of ω_c/ω_0 have been neglected. The same approximation has been used for further analysis. The second-order components of velocity (oscillating at the second harmonic of the radiation frequency) are generated due to the obliqueness of the uniform magnetic field and reduce to zero if the magnetic field is applied along the propagation direction, or is zero. The same procedure is used to obtain the third-order electron velocity components governed by

$$\frac{\partial v^{(3)}_{x,y,z}}{\partial t} + \frac{\partial}{\partial t}\left(\gamma^{(2)} v^{(1)}_{x,y,z}\right) + v^{(1)}_z \frac{\partial v^{(2)}_{x,y,z}}{\partial z} + v^{(2)}_z \frac{\partial v^{(1)}_{x,y,z}}{\partial z} = -\frac{e}{mc}(\vec{v}^{(2)} \times \vec{B})_{x,y,z} - \frac{e}{mc}\left(\vec{v}^{(3)} \times \vec{b}_0\right)_{x,y,z}. \tag{10}$$

Using Eqs. (7) and (9), simultaneous solution of Eq. (10) gives the third-order transverse velocities

$$v^{(3)}_x = -\frac{ca^3}{2\omega_0^2}\left[\omega_0^2 + 10\omega_c^2 + 4\omega_0\omega_c\cos\theta - \frac{21\omega_c^2\sin^2\theta}{4}\right]\sin(k_0 z - \omega_0 t) \tag{11a}$$

and

$$v^{(3)}_y = -\frac{ca^3}{2\omega_0^2}\left[\omega_0^2 + 10\omega_c^2 + 4\omega_0\omega_c\cos\theta - \frac{35\omega_c^2\sin^2\theta}{4}\right]\cos(k_0 z - \omega_0 t). \tag{11b}$$

While deriving Eqs. (11), harmonics of the laser frequency have been ignored.

The electron density is perturbed due to the interaction of the intense laser field with plasma. The first-order electron density is obtained by expanding the continuity Eq. (5) in orders of the radiation field. Thus

$$\frac{\partial n^{(1)}}{\partial t} + n^{(0)} \frac{\partial v^{(1)}_z}{\partial z} = 0, \tag{12}$$

where

$$n^{(0)} = n_0(r) = n_{00}\left(1 + \frac{\Delta n r^2}{n_{00} r_{ch}^2}\right)$$

is the unperturbed plasma electron density. It may be noted that the longitudinal velocity $v^{(1)}_z$, arising on account of the oblique magnetic field, generates first-order fluctuations in plasma density. Substituting the value of $v^{(1)}_z$ in Eq. (12) the first-order electron density perturbation is given by

$$n^{(1)} = -\frac{n_0(r) ca\omega_c k_0 \sin\theta(\omega_0 + \omega_c\cos\theta)}{\omega_0^3}\cos(k_0 z - \omega_0 t). \tag{13}$$

The first-order density perturbation arises due to the presence of the oblique external magnetic field and reduces to zero either if the field is switched off or is aligned along the direction of propagation of the laser beam. The second-order electron density perturbation may be obtained by solving the equation:

$$\frac{\partial n^{(2)}}{\partial t} + n^{(0)}\frac{\partial v^{(2)}_z}{\partial z} + n^{(1)}\frac{\partial v^{(1)}_z}{\partial z} + v^{(1)}_z \frac{\partial n^{(1)}}{\partial z} = 0 \tag{14}$$

as

$$n^{(2)} = \frac{n_0(r) c^2 a^2 \omega_c^2 k_0^2 \sin^2\theta}{2\omega_0^4}\cos 2(k_0 z - \omega_0 t). \tag{15}$$

The transverse components of the current density (upto the third order of the radiation field) are written as

$$J_{x,y} = -e\left(n^{(0)} v^{(1)}_{x,y} + n^{(0)} v^{(3)}_{x,y} + n^{(1)} v^{(2)}_{x,y} + n^{(2)} v^{(1)}_{x,y}\right).$$

It may be noted that the current density comprises of first and third-order terms only. The second-order terms ($n^{(1)}v^{(1)}$ and $n^{(0)}v^{(2)}$) oscillate at the second harmonic of the laser frequency and have therefore been neglected. Substitution of the

https://doi.org/10.1017/S0263034617000581 Published online by Cambridge University Press

plasma electron velocities and densities gives

$$J_x = -\frac{n_0(r)eca}{\omega_0^2}\Big[\omega_0(\omega_0+\omega_c\cos\theta)+\omega_c^2 - \frac{a^2}{2}\Big\{\omega_0^2+4\omega_0\omega_c\cos\theta+10\omega_c^2 + \frac{\omega_c^2\sin^2\theta}{4\omega_0^2}\left(2c^2k_0^2-21\omega_0^2\right)\Big\}\Big]\sin(k_0z-\omega_0t) \tag{16a}$$

and

$$J_y = -\frac{n_0(r)eca}{\omega_0^2}\Big[\omega_0(\omega_0+\omega_c\cos\theta)+\omega_c^2\cos^2\theta - \frac{a^2}{2}\Big\{\omega_0^2+4\omega_0\omega_c\cos\theta+10\omega_c^2 - \frac{\omega_c^2\sin^2\theta}{4\omega_0^2}\left(2c^2k_0^2+35\omega_0^2\right)\Big\}\Big]\cos(k_0z-\omega_0t). \tag{16b}$$

While deriving Eqs. (16), harmonics of the laser frequency have been neglected. It may be noted that the x- and y-components of current density are unequal in magnitude because the magnetic field lies in the y–z plane. This causes the component of the $\vec{v}\times\vec{b}_0$ force acting along the x-direction to be larger than that along the y-direction. The asymmetry in current density, arising due to the obliqueness of the external magnetic field, is expected to drive the amplitudes of the x and y-components of the laser field, with a quantitative difference. This point toward the possibility of conversion of the circularly polarized laser into an elliptically polarized beam.

3. WAVE DYNAMICS

The equations governing the evolution of the laser fields along the transverse directions are obtained by substituting Eqs. (16) into the wave Eq. (2), to give

$$\left[\nabla_\perp^2+\frac{\partial^2}{\partial z^2}-\frac{1}{c^2}\frac{\partial^2}{\partial t^2}\right]\vec{a}_1 = \frac{\omega_p^2}{c^2}\left[\frac{\left\{\omega_0(\omega_0+\omega_c\cos\theta)+\omega_c^2\right\}}{\omega_0^2}+\frac{\Delta nr^2}{n_{00}r_{ch}^2}\frac{\left\{\omega_0(\omega_0+\omega_c\cos\theta)+\omega_c^2\right\}}{\omega_0^2} - |a_1|^2Q_1-\frac{\Delta nr^2}{n_{00}r_{ch}^2}|a_1|^2Q_1\right]\vec{a}_1 \tag{17a}$$

and

$$\left[\nabla_\perp^2+\frac{\partial^2}{\partial z^2}-\frac{1}{c^2}\frac{\partial^2}{\partial t^2}\right]\vec{a}_2 = \frac{\omega_p^2}{c^2}\left[\frac{\left\{\omega_0(\omega_0+\omega_c\cos\theta)+\omega_c^2\cos^2\theta\right\}}{\omega_0^2} + \frac{\Delta nr^2}{n_{00}r_{ch}^2}\frac{\left\{\omega_0(\omega_0+\omega_c\cos\theta)+\omega_c^2\cos^2\theta\right\}}{\omega_0^2} - |a_2|^2Q_2-\frac{\Delta nr^2}{n_{00}r_{ch}^2}|a_2|^2Q_2\right]\vec{a}_2, \tag{17b}$$

where $\vec{a}_{1,2}$ are the laser fields along the x, y-directions and $\omega_p(=4\pi n_{00}e^2/m)^{1/2}$ is the plasma frequency while the coefficients

$$Q_1 = \frac{1}{2\omega_0^2}\left\{\omega_0^2+4\omega_0\omega_c\cos\theta+10\omega_c^2-\frac{\omega_c^2\sin^2\theta}{4\omega_0^2}\left(2\omega_p^2+19\omega_0^2\right)\right\}$$

and

$$Q_2 = \frac{1}{2\omega_0^2}\left\{\omega_0^2+4\omega_0\omega_c\cos\theta+10\omega_c^2-\frac{\omega_c^2\sin^2\theta}{4\omega_0^2}\left(37\omega_0^2-2\omega_p^2\right)\right\}$$

quantify the non-linear effects in obliquely magnetized plasma.

Considering only the linear terms on the right-hand side of Eqs. (17a) and (17b) leads to two linear dispersion relations for the x and y-components of the laser electric field, respectively as

$$c^2k_0^2 = \omega_0^2-\frac{\omega_p^2\left\{\omega_0(\omega_0+\omega_c\cos\theta)+\omega_c^2\right\}}{\omega_0^2} \tag{18a}$$

and

$$c^2k_0^2 = \omega_0^2-\frac{\omega_p^2\left\{\omega_0(\omega_0+\omega_c\cos\theta)+\omega_c^2\cos^2\theta\right\}}{\omega_0^2}. \tag{18b}$$

In the absence of obliqueness ($\theta = 0$) of the magnetic field, Eqs. (18) reduce to the well-known linear dispersion relation for a circularly polarized laser beam propagating in axially magnetized plasma (Jha *et al.*, 2007).

Assuming the radiation amplitude to be a slowly varying function of z, the term $\partial^2a_{1,2}/\partial z^2$ representing higher order diffraction effects is neglected in comparison with $2k_0\partial/\partial z$. Thus, the paraxial approximation of Eqs. (17) gives,

$$\left[\nabla_\perp^2+2ik_0\frac{\partial}{\partial z}\right]a_1(r,z) = -k_p^2\left[|a_1|^2Q_1+|a_1|^2Q_1\frac{\Delta nr^2}{n_{00}r_{ch}^2}-\frac{\left\{\omega_0(\omega_0+\omega_c\cos\theta)+\omega_c^2\right\}}{\omega_0^2} - \frac{\left\{\omega_0(\omega_0+\omega_c\cos\theta)+\omega_c^2\right\}}{\omega_0^2}\frac{\Delta nr^2}{n_{00}r_{ch}^2}\right]a_1(r,z) \tag{19a}$$

and

$$\left[\nabla_\perp{}^2+2ik_0\frac{\partial}{\partial z}\right]a_2(r,z) = -k_p^2\left[|a_2|^2Q_2+|a_2|^2Q_2\frac{\Delta nr^2}{n_{00}r_{ch}^2}-\frac{\left\{\omega_0(\omega_0+\omega_c\cos\theta)+\omega_c^2\cos^2\theta\right\}}{\omega_0^2} - \frac{\left\{\omega_0(\omega_0+\omega_c\cos\theta)+\omega_c^2\cos^2\theta\right\}}{\omega_0^2}\frac{\Delta nr^2}{n_{00}r_{ch}^2}\right]a_2(r,z). \tag{19b}$$

Since unequal current densities drive the x and y-components of the radiation field amplitude, the Lagrangian densities

https://doi.org/10.1017/S0263034617000581 Published online by Cambridge University Press

associated with the two equations Eqs. (19a) and (19b) are respectively written as

$$l_1 = \vec{\nabla}_\perp a_1^*.\vec{\nabla}_\perp a_1 + ik_0\left(a_1\frac{\partial a_1^*}{\partial z} - a_1^*\frac{\partial a_1}{\partial z}\right) - k_p^2\left[\frac{a_1^2 a_1^{*2}Q_1}{2} + \frac{a_1^2 a_1^{*2}Q_1}{2}\frac{\Delta n r^2}{n_{00}r_{ch}^2} - a_1 a_1^*\frac{\{\omega_0(\omega_0+\omega_c\cos\theta)+\omega_c^2\}}{\omega_0^2} - a_1 a_1^*\frac{\Delta n r^2}{n_{00}r_{ch}^2}\frac{\{\omega_0(\omega_0+\omega_c\cos\theta)+\omega_c^2\}}{\omega_0^2)}\right] \tag{20a}$$

and

$$l_2 = \vec{\nabla}_\perp a_2^*.\vec{\nabla}_\perp a_2 + ik_0\left(a_2\frac{\partial a_2^*}{\partial z} - a_2^*\frac{\partial a_2}{\partial z}\right) - k_p^2\left[\frac{a_2^2 a_2^{*2}Q_2}{2} + \frac{a_2^2 a_2^{*2}Q_2}{2}\frac{\Delta n r^2}{n_{00}r_{ch}^2} - a_2 a_2^*\frac{\{\omega_0(\omega_0+\omega_c\cos\theta)+\omega_c^2\cos^2\theta\}}{\omega_0^2} - a_2 a_2^*\frac{\Delta n r^2}{n_{00}r_{ch}^2}\frac{\{\omega_0(\omega_0+\omega_c\cos\theta)+\omega_c^2\cos^2\theta\}}{\omega_0^2}\right]. \tag{20b}$$

Considering a Gaussian radial profile, the trial functions representing the laser amplitudes may be written as

$$a_{1,2} = f_{1,2}(z)\exp\left(i\varphi_{1,2}(z) + \frac{i\alpha_{1,2}(z)r^2}{r_{s_{1,2}}^2(z)} - \frac{r^2}{r_{s_{1,2}}^2(z)}\right), \tag{21}$$

where $f_{1,2}(z)$, $\varphi_{1,2}(z)$, $\alpha_{1,2}(z)$, and $r_{s1,2}(z)$ are, respectively, the amplitude, phase shift, curvature and spot size corresponding to the laser field along the x and y-directions. Substituting Eq. (21) into (20) and using $\hat{l}_{1,2} = \int_0^\infty l_{1,2}rdr$, yields the reduced Lagrangian densities

$$\hat{l}_1 = \frac{(\alpha_1^2+1)f_1^2}{4} + \frac{f_1^2 r_{s1}^2 k_0}{4}\left[\frac{\partial\varphi_1}{\partial z} + \frac{1}{2}\frac{\partial\alpha_1}{\partial z} - \frac{\alpha_1}{r_{s1}}\frac{\partial r_{s1}}{\partial z}\right] + \frac{\{\omega_0(\omega_0+\omega_c\cos\theta)+\omega_c^2\}}{\omega_0^2}\frac{k_p^2 f_1^2 r_{s1}^2}{8} + \frac{k_p^2 f_1^2 r_{s1}^4\Delta n}{16 n_{00}r_{ch}^2} \times\frac{\{\omega_0(\omega_0+\omega_c\cos\theta)+\omega_c^2\}}{\omega_0^2} - \frac{3k_p^2 f_1^4 r_{s1}^2 Q_1}{128} - \frac{3k_p^2\Delta n f_1^4 r_{s1}^4 Q_1}{512 n_{00}r_{ch}^2} \tag{22a}$$

and

$$\hat{l}_2 = \frac{(\alpha_2^2+1)f_2^2}{4} + \frac{f_2^2 r_{s2}^2 k_0}{4}\left[\frac{\partial\varphi_2}{\partial z} + \frac{1}{2}\frac{\partial\alpha_2}{\partial z} - \frac{\alpha_2}{r_{s2}}\frac{\partial r_{s2}}{\partial z}\right] + \frac{\{\omega_0(\omega_0+\omega_c\cos\theta)+\omega_c^2\cos^2\theta\}}{\omega_0^2}\frac{f_2^2 r_{s2}^2 k_p^2}{8} + \frac{k_p^2\Delta n f_2^2 r_{s2}^4}{16 n_{00}r_{ch}^2} \times\frac{\{\omega_0(\omega_0+\omega_c\cos\theta)+\omega_c^2\cos^2\theta\}}{\omega_0^2} - \frac{3k_p^2 f_2^4 r_{s2}^2 Q_2}{128} - \frac{3k_p^2\Delta n f_2^4 r_{s2}^4 Q_2}{512 n_{00}r_{ch}^2}. \tag{22b}$$

Varying the reduced Lagrangian densities with respect to $\varphi_{1,2}(z)$ gives

$$\frac{\partial}{\partial z}\left(f_{1,2}^2 r_{s1,2}^2\right) = 0$$

or

$$f_{1,2}^2 r_{s1,2}^2 = f_0^2 r_0^2 = \text{constant}, \tag{23}$$

where f_0 and r_0 are the initial laser beam amplitude and spot size, respectively. Thus,

$$f_{1,2} = \frac{f_0 r_0}{r_{s1,2}}. \tag{24}$$

Variation with respect to curvature $\alpha_{1,2}(z)$ gives

$$\alpha_{1,2} = \frac{k_0 r_{s1,2}}{2}\frac{\partial r_{s1,2}}{\partial z}. \tag{25}$$

Similarly, varying Eqs. (22a) and (22b) with respect to spot size $r_{s1}(z)$ and $r_{s2}(z)$, respectively, leads to the equations governing the evolution of the spot size as,

$$\frac{\partial^2 r_{s1}}{\partial z^2} = \frac{4}{r_{s1}^3 k_0^2}\left[1 - \frac{3k_p^2 f_0^2 r_0^2 Q_1}{32} - \frac{k_p^2\Delta n r_{s1}^4}{4 n_{00}r_{ch}^2} \times\frac{\{\omega_0(\omega_0+\omega_c\cos\theta)+\omega_c^2\}}{\omega_0^2}\right] \tag{26a}$$

and

$$\frac{\partial^2 r_{s2}}{\partial z^2} = \frac{4}{r_{s2}^3 k_0^2}\left[1 - \frac{3k_p^2 f_0^2 r_0^2 Q_2}{32} - \frac{k_p^2\Delta n r_{s2}^4}{4 n_{00}r_{ch}^2} \times\frac{\{\omega_0(\omega_0+\omega_c\cos\theta)+\omega_c^2\cos^2\theta\}}{\omega_0^2}\right]. \tag{26b}$$

While deriving Eqs. (26), Eqs. (25) have been used. The first, second, and third terms on the right-hand side of Eqs. (26) represent vacuum diffraction, relativistic self-focusing and channel focusing of a laser beam in an obliquely magnetized plasma channel. It may be noted that relativistic self-focusing and channel focusing contributions to the evolution of the spot size of the laser beam along the x- and y-directions are not the same. Hence, the spot size r_{s1} and r_{s2} will evolve differently. If the laser spot size is considered to be matched, along one direction, it will remain mismatched along the other. The matching condition of the laser spot size along the y-direction as it propagates in the magnetized plasma channel is obtained by assuming that $r_{s2} = r_0, \partial r_{s2}/\partial z = 0$. With these conditions, Eq. (26b) gives the critical density gradient of the plasma channel for which the laser spot size along the y-direction remains matched ($r_{s2} = r_0$) as it propagates in a plasma channel, as

$$\Delta n_c = \frac{4 n_{00}r_{ch}^2\omega_0^2}{k_p^2 r_0^4\{\omega_0(\omega_0+\omega_c\cos\theta)+\omega_c^2\cos^2\theta\}} \times\left[1 - \frac{3k_p^2 f_0^2 r_0^2 Q_2}{32}\right]. \tag{27}$$

https://doi.org/10.1017/S0263034617000581 Published online by Cambridge University Press

It is seen that apart from other laser and plasma parameters, the critical channel density depends on the obliqueness (θ) of the applied magnetic field. For the same condition, the spot size along the x-direction (r_{s1}) remains mismatched. Solving Eqs. (24), (26), and (27) simultaneously, we can obtain the evolution of the spot size as well as the x- and y-amplitudes, with respect to the propagation distance. Since the amplitudes (f_1 and f_2) are expected to be unequal, the eccentricity of the laser beam polarization can be obtained from

$$\varepsilon = \sqrt{1 - \frac{f_2^2}{f_1^2}}. \tag{28}$$

It may be noted that the eccentricity will vary with the propagation distance.

4. NUMERICAL SOLUTIONS

In order to study the evolution of the laser spot size, it is interesting to first analyze the quiver velocities generated by the passage of the laser beam in the plasma channel, in the presence of the oblique magnetic field. The variation of the normalized (by c) amplitude of transverse quiver velocity components of plasma electrons (v_{0x} and v_{0y}) with the obliqueness of the magnetic field is shown in Figure 1. The modulus of the normalized initial, on-axis radiation field amplitude (a) is considered to be 0.2, $\sigma = +1$ and $\omega_c/\omega_0 = 0.08$ ($b_0 = 855T$). Curve *a (b)* represents the evolution of amplitude of the transverse quiver velocity component of the plasma electrons along the $x(y)$-direction. It is seen that when an axial ($\theta = 0°$) magnetic field is applied, the transverse quiver velocity components remain equal in magnitude along the x- and y-directions and are maximum. As the obliqueness (θ) of the magnetic field increases, these velocity components become unequal and also reduce. The asymmetry in the transverse quiver velocity components gives rise to unequal transverse current density components. Similarly, Figure 2 depicts the variation of the normalized amplitude of the longitudinal quiver velocity (v_{0z}) with the obliqueness (θ) of the external magnetic field, for the same parameters as in Figure 1. This curve shows that no longitudinal quiver velocity component is generated in case of axially ($\theta = 0°$) magnetized plasma. However, this velocity increases with an increase in the obliqueness of the external magnetic field. Also it may be noted that the amplitude of the transverse quiver velocity is about ten times larger than the longitudinal quiver velocity.

The evolution of the normalized spot size and amplitude of the laser beam propagating in an obliquely magnetized plasma channel is studied numerically by simultaneously solving Eqs. (24), (26), and (27), with the assumption that at $z = 0$, $\partial r_{s1,2}/\partial z = 0$ and $r_{s1,2} = r_0 = 25$ μm. The other laser, magnetic field, and plasma parameters are $f_0^2 = 0.04$ (Intensity $= 5.47 \times 10^{16}\mathrm{W/cm^2}$), $\lambda = 1$ μm, $\omega_c/\omega_0 = 0.08$, $n_{00} = 1.1 \times 10^{19}\mathrm{cm^{-3}}(\lambda_p = 10\ \mu\mathrm{m})$, and channel radius $r_{ch} = 40$ μm. The channel density gradient is considered to be equal to its critical value $\Delta n = \Delta n_c$ (Eq. (27)) for r_{s2}. Since Δn_c is a function of θ, its value for $\theta = 30°$, 45°, and 90° is respectively 1.71×10^{17}, 1.86×10^{17}, and $2.51 \times 10^{17}\mathrm{cm^{-3}}$. Figure 3 shows the simultaneous evolution of the normalized (by r_0) spot size of the laser beam with propagation distance, normalized by the Rayleigh length $Z_R(=\pi r_0^2/\lambda$ for an initially circularly polarized laser beam propagating in a magnetized plasma channel. Curves a, b, and c respectively, show the evolution of the spot size along the x-direction, when the applied magnetic field is at an angle $\theta = 30°$, 45°, and 90° with respect to the z-axis, while curve d represents the matched spot size along the

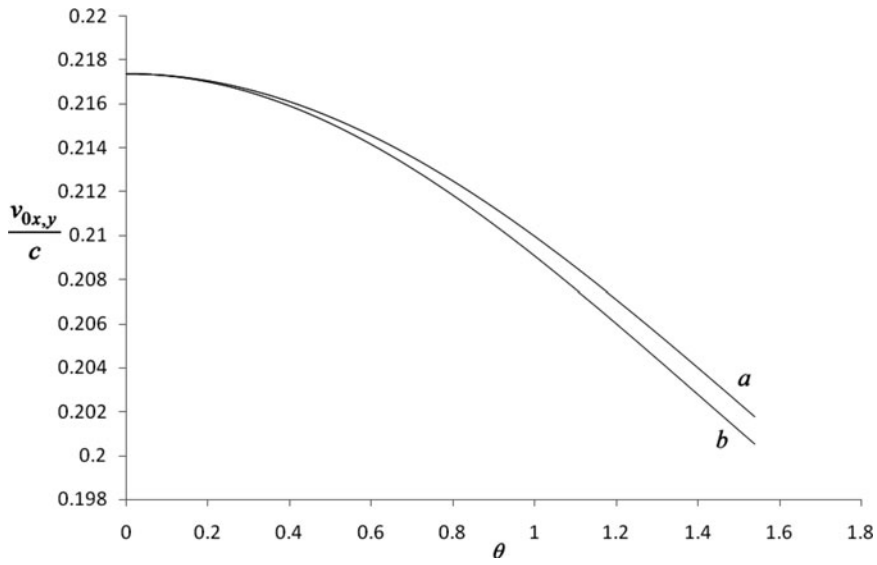

Fig. 1. Variation of the normalized amplitude of the transverse quiver velocities with obliqueness of the magnetic field (θ) for $a = 0.2$, $\sigma = +1$ and $\omega_c/\omega_0 = 0.08$. Curve $a(b)$ represents the amplitude of the transverse quiver velocity along the $x(y)$-direction.

https://doi.org/10.1017/S0263034617000581 Published online by Cambridge University Press

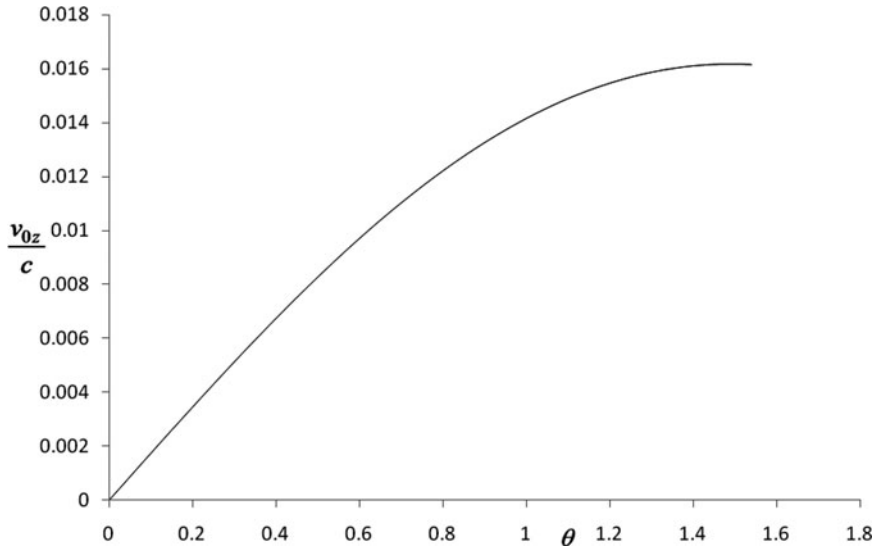

Fig. 2. Variation of the normalized amplitude of the longitudinal quiver velocity with obliqueness of the magnetic field (θ) for $a = 0.2$, $\sigma = +1$, and $\omega_c/\omega_0 = 0.08$. Curve represents the amplitude of the longitudinal quiver velocity along the z-direction.

y-direction. It is seen that the spot size along the x-direction is mismatched and oscillates with propagation distance. These betatron oscillations arising due to the presence of the plasma channel tend to confine the spot size. The beam spot size along the x-direction is mismatched because the obliqueness of magnetic field leads to asymmetric current densities along the transverse directions causing a significant enhancement in the relativistic as well as channel focusing along the x-direction, which in turn reduces the beam width along the x-direction as compared to the initial beam width. Comparison of curves a, b, and c, shows that the focusing effect enhances with the obliqueness (θ) of the magnetic field. After a certain propagation distance the spot size along the x-direction becomes equal to the spot size in the y-direction, implying that the beam spot attains a circular shape.

Figure 4 shows the simultaneous variation of the normalized amplitude of the x and y-components of the electric field of the laser beam, with normalized propagation distance, in an obliquely magnetized plasma channel, for the same parameters as in the case of Figure 1. The curves a, b, and c, respectively, show the evolution of the amplitude of the x component, for $\theta = 30°$, 45°, and 90° while curve d represents the y component amplitude, under matching conditions. These curves show a reverse trend as compared to those in Figure 1, since the evolution of the amplitude depends

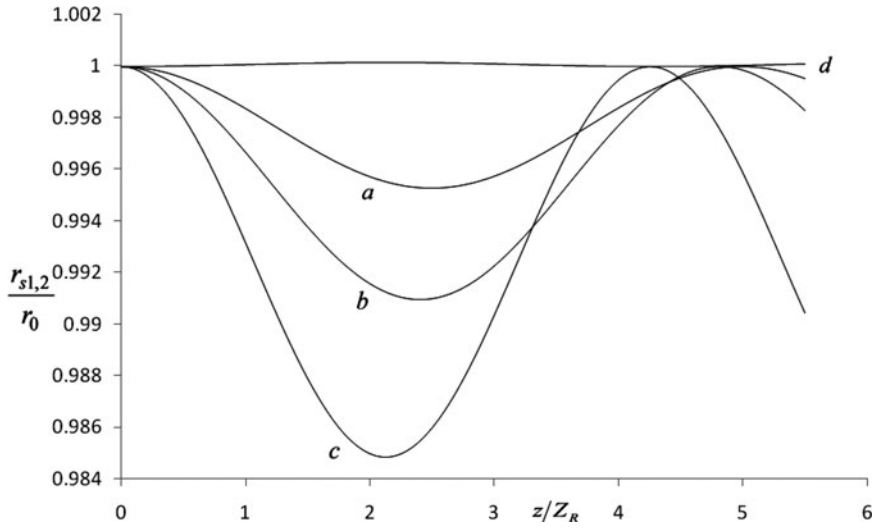

Fig. 3. Variation of normalized spot size of a laser beam with normalized propagation distance for $r_{ch} = 40$ μm, $\lambda = 1$ μm, $f_0^2 = 0.04$, $r_0 = 25$ μm, $n_{00} = 1.1 \times 10^{19}\text{cm}^{-3}$, and $\omega_c/\omega_0 = 0.08$. Curves *a, b* and *c* represent the spot size along the x-direction for $\theta = 30°$ ($\Delta n_c = 1.71 \times 10^{17}\text{cm}^{-3}$), $\theta = 45°$ ($\Delta n_c = 1.86 \times 10^{17}\text{cm}^{-3}$), and $\theta = 90°$ ($\Delta n_c = 2.51 \times 10^{17}\text{cm}^{-3}$), respectively. Curve *d* depicts the matched spot size along the y-direction for all values of θ.

https://doi.org/10.1017/S0263034617000581 Published online by Cambridge University Press

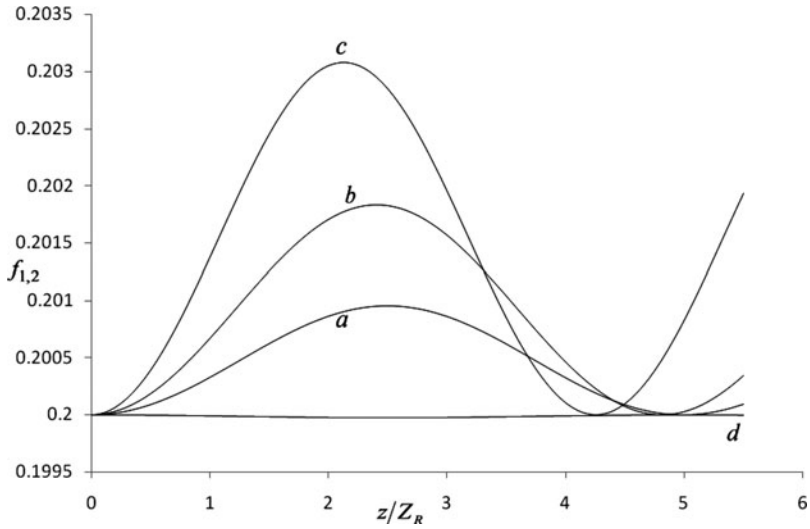

Fig. 4. Variation of normalized amplitude of a laser beam with normalized propagation distance for $r_{ch} = 40$ μm, $\lambda = 1$ μm, $f_0^2 = 0.04$, $r_0 = 25$ μm, $n_{00} = 1.1 \times 10^{19}\text{cm}^{-3}$, and $\omega_c/\omega_0 = 0.08$. Curves *a*, *b*, and *c* represent the amplitude of electric field along the *x*-direction for $\theta = 30°$ ($\Delta n_c = 1.71 \times 10^{17}\text{cm}^{-3}$), $\theta = 45°$ ($\Delta n_c = 1.86 \times 10^{17}\text{cm}^{-3}$), and $\theta = 90°$ ($\Delta n_c = 2.51 \times 10^{17}\text{cm}^{-3}$), respectively. Curve *d* depicts the matched amplitude of electric field along the *y*-direction for all values of θ.

inversely on the spot size. The amplitude of the electric field along the *x* and *y*-directions, which was initially equal (circularly polarized) starts becoming unequal (elliptically polarized), as the laser beam propagates in plasma. Thus, obliquely magnetized plasma channel can convert a circularly polarized laser beam into an elliptically polarized beam and works as a quarter wave plate.

Figure 5 depicts the evolution of eccentricity [Eq. (28)] of the polarization of the laser beam propagating in a magnetized plasma channel. All parameters are the same as in Figure 1. Curves *a*, *b*, and *c*, respectively, show the variation of eccentricity of the laser beam when the beam propagates in a plasma channel embedded in an obliquely applied magnetic field. These curves show that the eccentricity of the laser beam changes with propagation distance. The eccentricity attains a maximum value of 0.099, 0.135, and 0.174 (at $2.5Z_R$, $2.4Z_R$, and $2.15Z_R$) for $\theta = 30°$, 45°, and 90°, respectively. After the beam has traversed a certain distance the eccentricity decreases sharply, due to the rapid decrease in the *x* amplitude of the laser beam. Thus, elliptically polarized laser beams of desired eccentricity can be obtained, by choosing appropriate values of the magnetic field, angle θ and propagation distance. It may also be noted that eccentricity increases with the obliqueness (θ) of applied magnetic field.

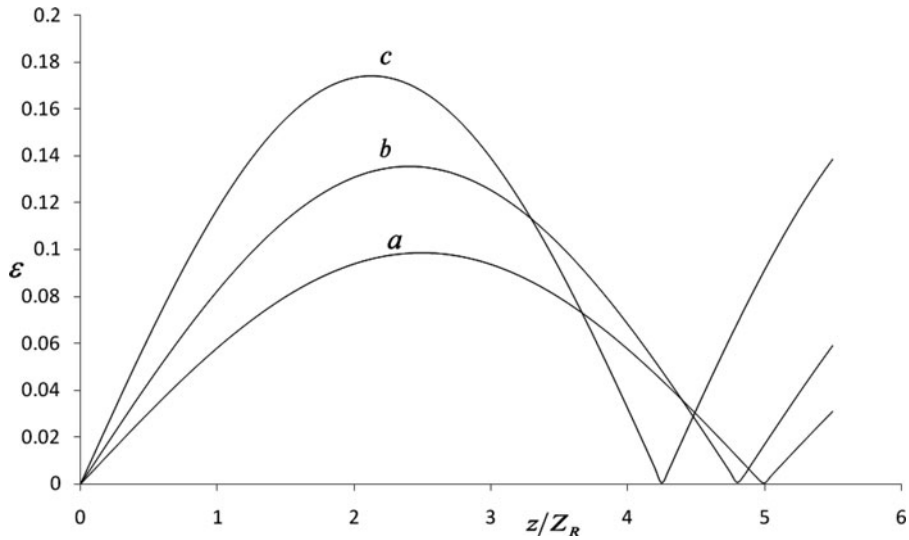

Fig. 5. Variation of eccentricity of a laser beam with normalized propagation distance for $r_{ch} = 40$ μm, $\lambda = 1$ μm, $f_0^2 = 0.04$, $r_0 = 25$ μm, $n_{00} = 1.1 \times 10^{19}\text{cm}^{-3}$, and $\omega_c/\omega_0 = 0.08$. The curves *a*, *b*, and *c*, respectively, depict the evolution of eccentricity for $\theta = 30°$ ($\Delta n_c = 1.71 \times 10^{17}\text{cm}^{-3}$), $\theta = 45°$ ($\Delta n_c = 1.86 \times 10^{17}\text{cm}^{-3}$), and $\theta = 90°$ ($\Delta n_c = 2.51 \times 10^{17}\text{cm}^{-3}$).

https://doi.org/10.1017/S0263034617000581 Published online by Cambridge University Press

Therefore, the maximum eccentricity is obtained when the applied magnetic field is applied along the transverse ($\theta = 90°$) direction. It is seen that eccentricity becomes zero at $5.0Z_R$, $4.75Z_R$, and $4.3Z_R$ for $\theta = 30°$, 45°, and 90°, respectively. At these distances the laser beam becomes circularly polarized again. Thus, extracting the laser beam at appropriate distances allows the obliquely magnetized plasma channel to convert laser beams having circular into elliptical polarization and can serve as a retarder.

5. SUMMARY AND CONCLUSIONS

Non-linear propagation of a circularly polarized laser beam, in a preformed, obliquely magnetized plasma channel having a parabolic density profile, has been analyzed. The external magnetic field is applied in the y–z plane. Using perturbation technique, plasma electron velocities, and densities are obtained. It is observed that when the magnetic field is applied along the axis, the transverse quiver velocity components along the x- and y-directions remain equal and are the maximum, while these velocity components become unequal and reduce with the obliqueness of external magnetic field. It may be also noted that a new longitudinal velocity component is generated. This velocity increases with the obliqueness of the applied external magnetic field. The obliquely applied magnetic field leads to the generation of unequal current densities along the two transverse directions. The laser field equations governing the propagation of the laser beam in an obliquely magnetized plasma channel have been set up. Lagrangian method has been used to derive the evolution equations of the laser spot size and amplitude of x- and y-components of the electric vector. The spot size as well as the amplitude of the laser electric field, along the two transverse directions, is seen to be asymmetrical. In order to study the evolution of the laser beam, the channel depth is chosen such that the spot size along the y-direction is matched. It is seen that although the spot size remains matched along the y-direction, the spot size along the x-direction is mismatched and oscillates with the propagation distance. The focusing effect is sharply enhanced with the obliqueness of external magnetic field. The field amplitude of the laser beam along the two transverse directions shows a reverse trend. At certain propagation distances, the beam amplitudes along the two transverse directions are unequal. This implies that the polarization of the laser field becomes elliptical. The eccentricity of the elliptically polarized laser beams varies continuously in the plasma channel. Therefore, we can obtain elliptically polarized laser beams of desired eccentricity, by choosing appropriate values of the magnetic field, angle θ and propagation distance. It is also observed that eccentricity increases with the obliqueness (θ) of the applied magnetic field and is the maximum for transversely applied magnetic field. This study provides an estimate for the changes not only in laser parameters but also in the state of polarization with the propagation distance. Thus, obliquely magnetized plasma channel can convert the polarization of a laser beam from circular to elliptical and may serve as a retardation device.

REFERENCES

Abdelli, S., Khalfaoui, A., Kerdja, T. & Ghobrini, D. (1992). Laser-plasma interaction properties through second harmonic generation. *Laser Part. Beams* **10**, 629–637.

Amendt, P., Eder, D.C. & Wilks, S.C. (1991). X-ray lasing by optical field induced ionization. *Phys. Rev. Lett*. **66**, 2589–2592.

Berezhiani, V. I. & Murusidze, I.G. (1992). Interaction of highly relativistic short laser pulses with plasmas and nonlinear wakefield generation. *Phys. Scr*. **45**, 87–90.

Chen, H.-Y., Liu, S.-Q. & Li, X.-Q. (2011). Self-modulation instability of an intense laser beam in a magnetized pair plasma. *Phys. Scr*. **83**, 035502.

Deutsch, C., Furukaw, H., Mima, K., Murakami, M. & Nishihara, K. (1996). Interaction physics of fast ignitor concept. *Phys. Rev. Lett*. **77**, 2883–2486.

Eder, D.C., Amemdt, P., Dasilva, L.B., London, R.A., Macgowan, B.J., Matthews, D.L., Penetrquante, B.M., Rosen, M.D., Wilks, S.C., Donnelly, T.D., Falcone, R.W. & Strobel, G.L. (1994). Tabletop x-ray lasers. *Phys. Plasmas* **1**, 1744–1752.

Esarey, E., Schroeder, C.B. & Leemans, W.P. (2009). Physics of laser-driven plasma-based electron accelerators. *Rev. Mod. Phys*. **81**, 1229.

Esarey, E., Sprangle, P., Krall, J. & Ting, A. (1996). Overview of plasma based accelerator concepts. *IEEE Trans. Plasma Sci*. **24**, 252–288.

Esarey, E., Sprangle, P., Krall, J. & Ting, A. (1997). Self- focusing and guiding of short laser pulses in ionizing gases and plasmas. *IEEE J. Quant. Electron*. **33**, 1879–1914.

Gorbunov, L.M., Mora, P. & Antonsen Jr., T.M. (1997). Quasistatic magnetic field generated by a short laser pulse in an underdense plasma. *Phys. Plasmas* **4**, 4358–4368.

Hu, Z.D., Sheng, Z.M., Ding, W.J., Wang, W.M., Dong, Q.L. & Zhang, J. (2012). Electromagnetic emission from laser wakefields in underdense magnetized plasmas. *J. Plasma Phys*. **78**, 421–427.

Hu, Z.D., Sheng, Z.M., Ding, W.J., Wang, W.M., Dong, Q.L. & Zhang, J. (2013). Probing the laser wakefield in underdense plasmas by induced terahertz emission *Phys*. *Plasmas* **20**, 080702.

Jha, P., Hemlata & Misra, R.K. (2014). Evolution of chirped laser pulses in a magnetized plasma channel. *Phys. Plasmas* **21**, 123106.

Jha, P., Kumar, P., Raj, G. & Upadhyay, A.K. (2005). Modulation instability of laser pulse in magnetized plasma. *Phys. Plasmas* **12**, 123104.

Jha, P., Mishra, R.K., Raj, G. & Upadhyay, A.K. (2007). Second harmonic generation in laser magnetized-plasma interaction. *Phys. Plasmas* **14**, 053107.

Jha, P., Mishra, R.K., Upadhyay, A.K. & Raj, G. (2006). Self-focusing of intense laser beam in magnetized plasma. *Phys. Plasmas* **13**, 103102.

Jha, P., Mishra, R.K., Upadhyay, A.K. & Raj, G. (2007). Spot-size evolution of laser beam propagating in plasma embedded in axial magnetic field. *Phys. Plasmas* **14**, 114504.

Jha, P., Saroch, A., Misra, R.K. & Upadhayay, A.K. (2012). Laser wakefield acceleration in magnetized plasma. *Phys. Rev. ST – A&B* **15**, 081301/1-6.

https://doi.org/10.1017/S0263034617000581 Published online by Cambridge University Press

Kaw, P., Schmidt, G. & Wilcox, T. (1973). Filamentation and trapping of electromagnetic radiation in plasmas. *Phys. Fluid* **16**, 1522.

Manouchehrizadeh, M. & Dorranian, D. (2013). Effect of obliqueness of external magnetic field on the characteristics of magnetized plasma wakefield. *J. Theor. Appl. Phys*. **7**, 43.

Nuzzo, S., Zarcone, M., Ferrante, G. & Basile, S. (2000). A simple model of high harmonic generation in a plasma. *Laser Part. Beams* **18**, 483–487.

Ren, C. & Mori, W.B. (2004). Nonlinear and three-dimensional theory for cross-magnetic field propagation of short-pulse lasers in underdense plasmas. *Phys. Plasmas* **11**, 1978.

Sharma, P., Wadhwani, N. & Jha, P. (2017). Terahertz radiation generation by propagation of circularly polarized laser pulses in axially magnetized plasma. *Phys. Plasmas* **24**, 013102.

Shen, Y.R. (1984). *The Principle of Nonlinear Optics*. New York: Wiley.

Tabak, M., Hammer, J., Glinsky, M.E., Kruer, W.L., Wilks, S.C., Woodworth, J., Campbell, E.M., Perry, M.D. & Mason, R.J. (1994). Ignition and high gain with ultrapowerful lasers. *Phys. Plasmas* **1**, 1626–1634.

Tajima, T. & Dawson, J. M. (1979). Laser electron accelerator. *Phys. Rev. Lett*. **43**, 267–270.

Verma, N.K. & Jha, P. (2016). Enhanced terahertz radiation generation by two-color laser pulses propagating in plasma. *Laser Part. Beams* **34**, 378–383.

Wang, W.-M., Gibbon, P., Sheng, Z.-M. & Li, Y.-T. (2015). Tunable circularly polarized terahertz radiation from magnetized gas plasma. *Phys. Rev. Lett*. **114**, 253901/1-5.